

pubs.acs.org/JPCL Letter

Excitation Energy Dependence of Photoluminescence Quantum Yields in Semiconductor Nanomaterials with Varying Dimensionalities

William M. Sanderson,[†] Jessica Hoy,[†] Calynn Morrison, Fudong Wang, Yuanyuan Wang, Paul J. Morrison, William E. Buhro, and Richard A. Loomis*



Cite This: J. Phys. Chem. Lett. 2020, 11, 3249-3256



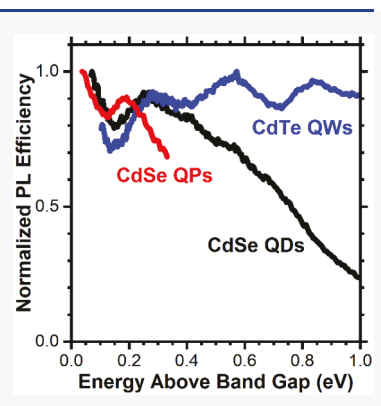
ACCESS

Metrics & More

Article Recommendations

Supporting Information

ABSTRACT: The excitation energy dependence (EED) of the photoluminescence quantum yield (Φ_{PL}) of semiconductor nanoparticles with varying dimensionalities is reported. Specifically, the EEDs of CdSe quantum dots, CdSe quantum platelets, CdSe quantum belts, and CdTe quantum wires were determined via measurements of individual Φ_{PL} values and photoluminescence efficiency $(PL_{Eff}(E))$ spectra. There is a general trend of overall decreasing efficiency for radiative recombination with increasing excitation energy. In addition, there are often local minima in the $PL_{Eff}(E)$ spectra that are most often at energies between quantum-confinement transitions. The average PL lifetimes of the samples do not depend on the excitation energy, suggesting that the EED of Φ_{PL} arises from charge carrier trapping that competes efficiently with intraband carrier relaxation to the band edge. The local minima in the $PL_{Eff}(E)$ spectra are attributed to excitation into optically coupled states that results in the loss of carriers in the semiconductor. The EED data suggest that the $PL_{Eff}(E)$ spectra depend on the sample synthesis, preparation, surface passivation, and environment.



emiconductor nanoparticles (NPs) have been extensively studied for their abilities to absorb and emit photons across a tunable range of the electromagnetic spectrum due to quantum-confinement effects. 1-7 The photoluminescence (PL) quantum yield (Φ_{PL}) of a sample is a useful metric for assessing the overall quality of the NPs, optimizing synthetic procedures, and improving device efficiencies that incorporate NPs. The $\Phi_{\rm PL}$ is the ratio of emission to absorption events. The absorption of a photon promotes excited charge carriers that ultimately dissipate the excess excitation energy via radiative or nonradiative mechanisms. In an ideal semiconductor NP, excited charge carriers relax within the conduction band (CB) and valence band (VB) to the lowest-energy quantum-confinement states. Because of the large energetic band gap between the CB and VB states, the carriers in an ideal semiconductor NP would recombine through radiative recombination and the Φ_{PL} value would be

When electrons and holes are initially prepared at the band edge in typical semiconductor NPs, the carriers may interact with a variety of nonradiative sources, including surface states, $^{8-11}$ crystallographic defects, $^{12-14}$ ligand transfer, 15,16 and environmental quenching. 15,17,18 The extent to which nonradiative pathways affect the $\Phi_{\rm PL}$ of a sample is therefore dependent on the crystalline quality and surface passivation. In practice, near-unity $\Phi_{\rm PL}$ values are rarely obtained for NPs without extensive surface modifications, such as the incorporation of protective semiconducting shell materials. $^{19-27}$

The absorption of a highly energetic photon creates charge carriers with energies in excess of the NP band gap, and this excess kinetic energy must be dissipated prior to reaching the band edge. Mechanisms for intraband relaxation include phonon coupling, $^{28-30}$ nonadiabatic transitions, 31 or Augermediated pathways. $^{28,32-34}$ Although relaxation to the band edge typically occurs on the subpicosecond to picosecond time scale in semiconductor NPs, 28,35,36 fast carrier-trapping pathways have been proposed to compete with intraband relaxation. 23,37,38 Since the $\Phi_{\rm PL}$ of an NP is sensitive to all nonradiative processes that occur, the specific energetic states in which the electrons and holes are prepared and the total of the nonradiative pathways that the charge carriers may sample can give rise to an excitation energy dependence (EED) of the $\Phi_{\rm PL}$.

We previously reported the EED of the emission efficiency of CdSe and CdSe/ZnS quantum dots (QDs) measured in two complementary ways. The first method involved direct measurements of the $\Phi_{\rm PL}$ values at discrete excitation energies E to obtain the $\Phi_{\rm PL}(E)$ spectrum as a function of excitation

Received: February 13, 2020 Accepted: April 7, 2020 Published: April 7, 2020





energy. The second method quantified the EED by measuring the quantum yield efficiency, $\Phi_{\rm Eff}(E)$, spectrum. In this method, the absorption, ${\rm Abs}(E)$, and photoluminescence excitation, ${\rm PLE}(E)$, spectra were collected. The photoluminescence efficiency, ${\rm PL}_{\rm Eff}(E)$, spectrum is the ratio of the ${\rm PLE}(E)$ to the absorptance spectrum, or equivalently,

$$PL_{Eff}(E) = \frac{PLE(E)}{1 - 10^{-Abs(E)}}$$
(1)

The $\operatorname{PL}_{\operatorname{Eff}}(E)$ spectrum can then be scaled using Φ_{PL} values measured at discrete excitation energies to yield a $\Phi_{\operatorname{Eff}}(E)$ spectrum for each sample. Hoy et al. 23 reported that the $\Phi_{\operatorname{Eff}}(E)$ spectra are in good agreement with numerous individual Φ_{PL} values measured across a broad range of excitation energies. An advantage of using the $\operatorname{PL}_{\operatorname{Eff}}(E)$ or $\Phi_{\operatorname{Eff}}(E)$ spectra to quantify the EED of the PL efficiency is that it allows for rapid data collection in comparison to the meticulous collection of a series of Φ_{PL} values at many different excitation energies.

For CdSe QDs, we observed an overall decrease in the $\Phi_{\rm Eff}(E)$ spectrum with increasing excitation energy as well as several local minima. The $\Phi_{\rm Eff}(E)$ spectrum for CdSe/ZnS QDs exhibited a similar decrease with increasing excitation energy, but there were no local minima present. Mooney et al. also measured the efficiency spectra of CdSe QDs. Those spectra contained several prominent minima, but there was a negligible overall change in efficiency with increasing excitation energy. The $PL_{\rm Eff}(E)$ collected for other samples of CdSe QDs contained both minima and decreasing PL efficiencies with increasing excitation energy. These latter EED trends are consistent the results obtained for various QD systems $^{16,38,40-43}$ and perovskite NPs. 38,44

To date, studies on the EED of the PL efficiency have primarily focused on zero-dimensional (0D) QDs, which have a discrete density of quantum-confinement states. Elongated NPs with increased dimensionality, such as one-dimensional (1D) quantum wires (QWs) and pseudo-1D quantum platelets (QPs) and quantum belts (QBs), have an increased density of states (DOS) due to the elongation of the NPs and the opening of a translational degree of freedom for the carriers. The resultant DOS in QWs is sawtoothlike, while the DOS in pseudo-1D QPs and QBs depends explicitly on their size in each dimension, and they may have 1D sawtoothlike or 2D steplike distributions. The larger DOS in these nanomaterials may affect the relaxation mechanisms and efficiencies for carrier relaxation dynamics.

In this Letter, we report the $PL_{Eff}(E)$ spectra for several types of II–VI semiconductor NPs. Specifically, colloidal samples of wurtzite (W) CdSe QDs (~4.1 and 5.7 nm in diameter), W CdSe QPs (~1.8 nm in thickness, ~10 nm in width, and ~50 nm in length), W CdSe QBs (~1.8 nm in thickness, ~10 nm in width, and >300 nm in length), W CdTe QWs (6.0 nm in diameter and 1–10 μ m in length), and enhanced CdTe QWs (7.4 and 7.5 nm in diameter and 1–10 μ m in length) with mixed zinc blende/wurtzite (ZB/W) and predominantly W crystal structures, respectively. A two-step thermal–photoexcitation process 46 was implemented to significantly improve the surface passivation and the Φ_{PL} of the as-synthesized CdTe QWs and to obtain samples of enhanced CdTe QWs. See Supporting Information section 1 (SI §1) for more details of the NP syntheses.

Extinction spectra of these NPs were collected, and particular attention was paid to removal of any scattering components in order to obtain the Abs(E) spectra of the NPs, as described in SI §2. Care was also taken either to account for absorption contributions from ligands or solvent molecules in the samples or to avoid analyzing spectral regions where these contributions are significant. The Abs(E) spectra (black spectra in Figure 1) contain features or local maxima

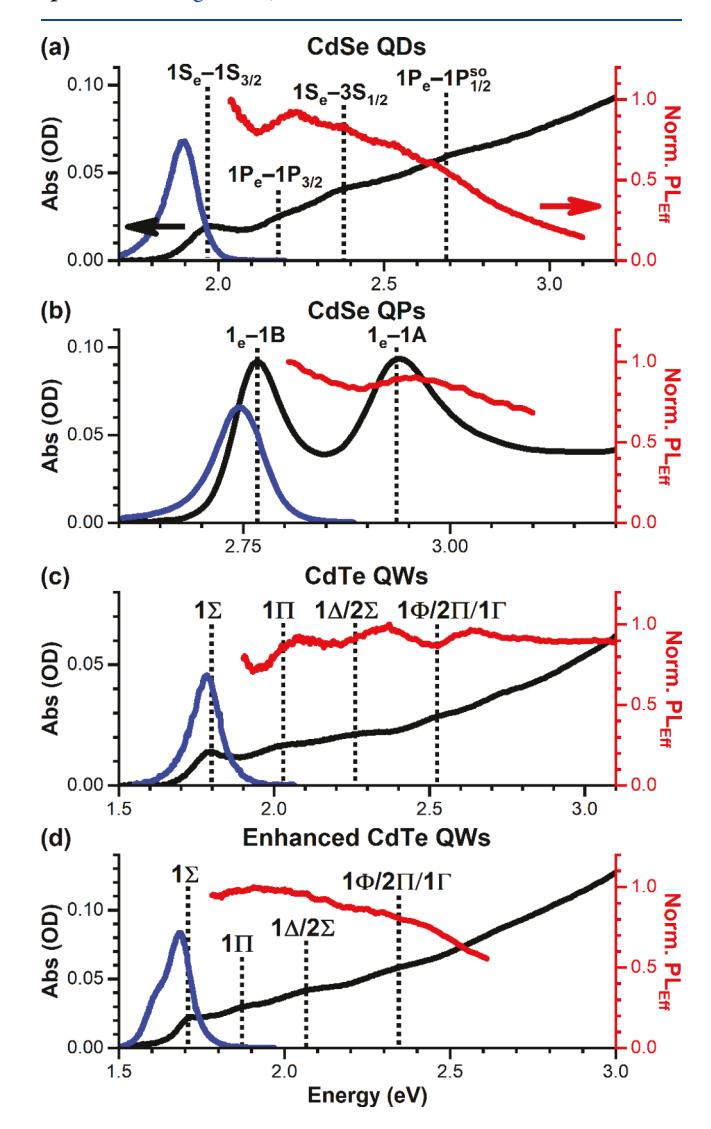


Figure 1. Absorption (Abs(E), black), photoluminescence (PL(E), blue), and photoluminescence efficiency (PL_{Eff}(E), red) spectra for (a) W CdSe QDs (5.7 nm diameter) in toluene, (b) W CdSe QPs (~1.8 nm thick) in toluene/oleylamine (1:1 v/v), (c) W CdTe QWs (6.0 nm diameter) in tri-n-octylphosphine, and (d) enhanced ZB/W CdTe QWs (7.4 nm diameter) in tri-n-octylphosphine. Peak energies of quantum-confinement states are plotted as dotted lines.

associated with transitions or groups of transitions between quantum-confinement states of the electron in the CB and the hole in the VB. The energies of prominent absorption features were determined using second-derivative analyses, as described in SI §3, and the results are listed in Table SI. The spectral assignments for the features within the spectra of the CdSe QDs and CdSe QPs are included in Figure 1, but because of mixing of the quantum-confinement states in the VB of the

CdTe QWs,⁴⁷ only the states accessed in the CB are used as labels in Figure 1c,d.

The PLE(E) spectrum of each sample was recorded so that the corresponding PL_{Eff}(E) spectra could be obtained using eq 1. Since the shapes of the PL(E) spectra of the NP samples (blue spectra in Figure 1) do not change with excitation energy, any features observed in the PL_{Eff}(E) spectra cannot be attributed to issues with the collection of the PLE(E) spectra as described in SI §2. The PL_{Eff}(E) spectra (red) for these four NPs, normalized to unity, are included in Figure 1. The trends observed in the PL_{Eff}(E) spectra were verified by separately measuring $\Phi_{\rm PL}$ values at numerous excitation energies (Figure S18). For reference, $\Phi_{\rm PL}=27.5\%$ was measured using excitation at 2.230 eV for the CdSe QPs, $\Phi_{\rm PL}=17.5\%$ was measured at 2.883 eV for the CdSe QPs, $\Phi_{\rm PL}=0.16\%$ was measured at 2.850 eV for the CdTe QWs, and $\Phi_{\rm PL}=13.5\%$ was measured at 1.922 eV for the enhanced CdTe QWs.

There is clearly an EED of the PL efficiency for each NP sample, as the values in the $PL_{Eff}(E)$ spectra do not remain constant with excitation energy. There is a prominent minimum just above the band-edge energy in the $PL_{Eff}(E)$ spectra of the CdSe QDs, CdSe QPs, and CdTe QWs. Additional minima are observed at higher energies for the CdSe QDs and CdTe QWs. A second-derivative analysis was performed on each $PL_{Eff}(E)$ spectrum to identify the energies of the minima, and the values are listed in Table SI. There are also notable decreases in the efficiencies for the CdSe QDs and CdSe QPs with increasing excitation energy. The $PL_{Eff}(E)$ spectrum of the enhanced CdTe QWs increases slightly and then decreases with excitation energy with no discernible local minima. Unfortunately, we could not record reliable data to even higher energies for any of the samples because of overlapping ligand or solvent absorption.

The additional energy imparted to the carriers with increasing excitation energy could affect the dynamics of the carriers in the states close to the band edge. These dynamics would have to include an increase in the nonradiative processes at the band edge in order to yield a decrease in PL efficiency with increasing energy. These processes would result in changes in the lifetimes of the carriers at the band edge and of the time-resolved PL decay (TRPLD) profiles recorded at different energies using pulsed excitation. The PL lifetime ($\tau_{\rm PL}$) can be measured by fitting each TRPLD profile to an exponential decay. If no nonradiative processes are incurred during intraband relaxation of the carriers, the $\Phi_{\rm PL}$ value at each excitation energy would then change with $\tau_{\rm PL}$ according to 48

$$\Phi_{\rm PL} \propto \frac{\tau_{\rm PL}}{\tau_{\rm rad}} \cdot 100\% \tag{2}$$

where $\tau_{\rm rad}$ is the radiative lifetime of the NP. An increase in the contributions from nonradiative, nonreversible pathways would result in a decrease in $\tau_{\rm PL}$ and a reduction in $\Phi_{\rm PL}$. Although the TRPLD profiles of semiconductor NPs are often multiexponential, the same trend would be observed; a decrease in the average decay lifetime, $\tau_{\rm AVG}$, would result in a decrease in $\Phi_{\rm PL}$.

To investigate this possibility, the TRPLD profiles and Φ_{PL} values for several NP samples were measured as a function of excitation energy. The TRPLDs were recorded by detection of emission at the maximum of the PL(E) spectrum using low excitation fluences to minimize the effects of multicarrier interactions. The Abs(E) and PL(E) spectra along with the

TRPLDs collected for these samples are shown in Figures S19–22. The TRPLD profiles are multiexponential, and each was fit to a sum of exponentials. From the fit parameters, listed in Tables SII–SV, a $\tau_{\rm AVG}$ for each excitation energy was calculated. The $\Phi_{\rm PL}$ and $\tau_{\rm AVG}$ values obtained for each sample are plotted in Figure 2. Although significant decreases in the

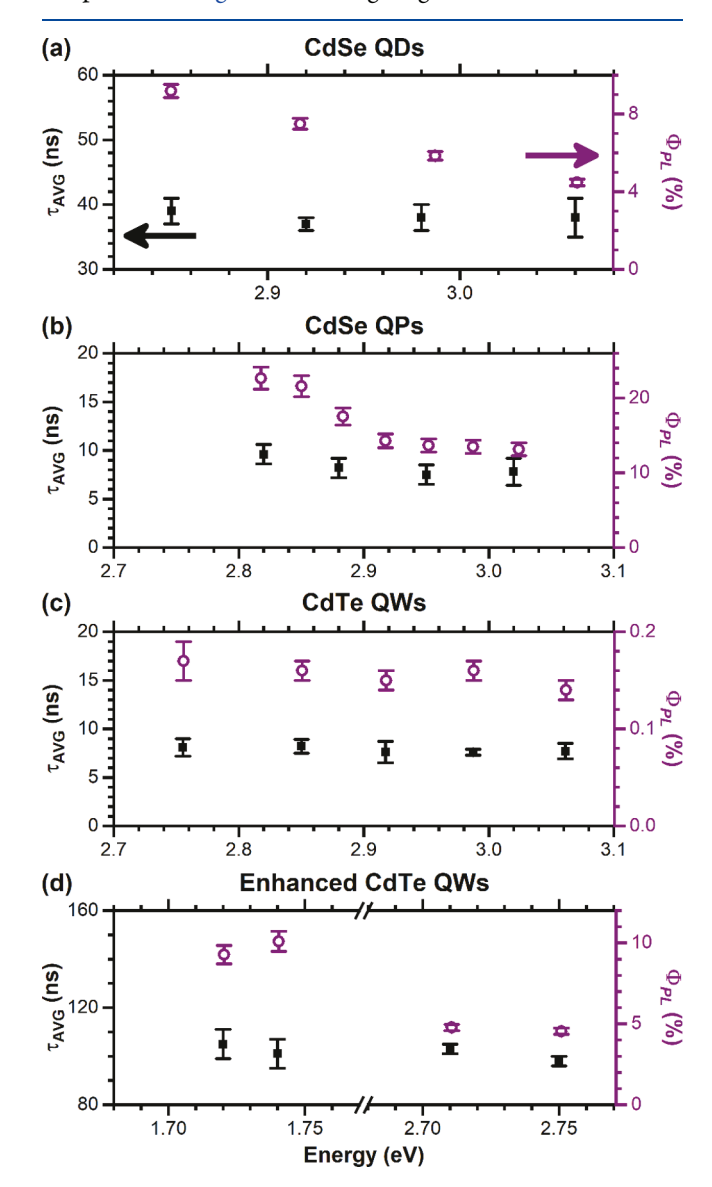


Figure 2. Comparison of $\tau_{\rm AVG}$ (black solid squares) and $\Phi_{\rm PL}$ (purple open circles) values measured at multiple excitation energies for (a) W CdSe QDs (5.7 nm diameter) in toluene, (b) W CdSe QPs (\sim 1.8 nm thick) in toluene/oleylamine (1:1 v/v), (c) W CdTe QWs (6.0 nm diameter) in tri-n-octylphosphine, and (d) enhanced ZB/W CdTeQWs (7.4 nm diameter) in tri-n-octylphosphine.

 $\Phi_{\rm PL}$ values were measured with increasing excitation energy, no appreciable changes in $\tau_{\rm AVG}$ were identified for any of these samples. The nearly constant $\tau_{\rm AVG}$ for each sample indicates that the dynamics at the band edge does not depend on the excitation energy. Instead, the decreasing PL efficiency with increasing excitation energy observed for a majority of the samples investigated arises because charge carriers access nonradiative pathways during relaxation to the band edge.

The schematic in Figure 3a illustrates how a continuum of carrier trap states, or nonradiative relaxation pathways, would

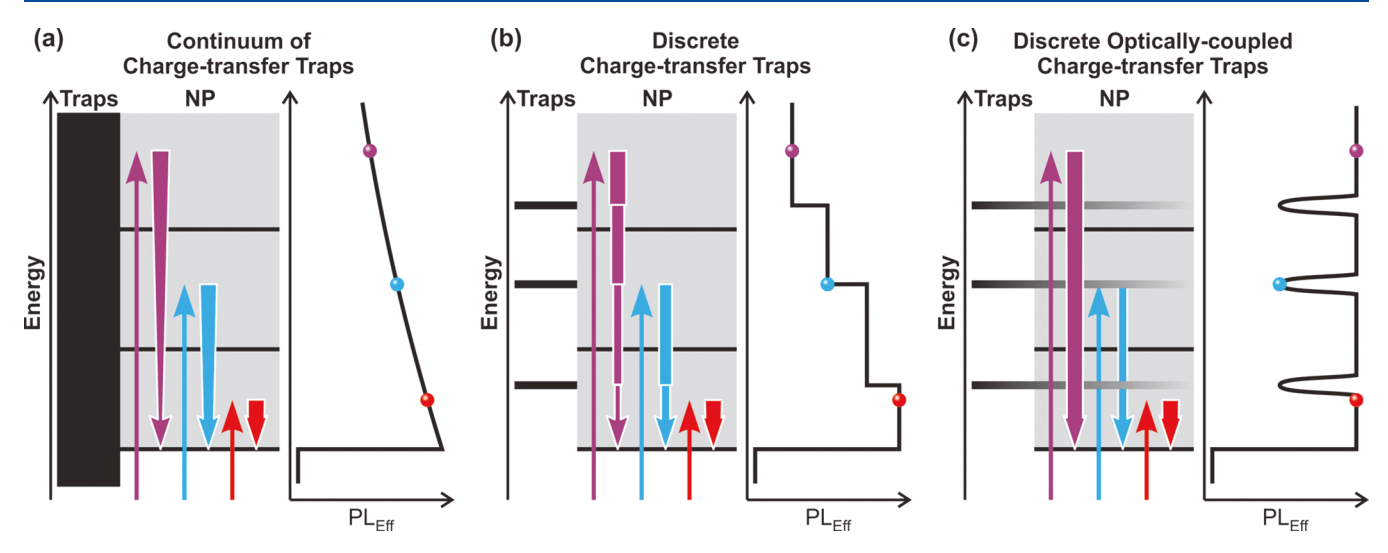


Figure 3. Three electron-trapping mechanisms that would yield contrasting $PL_{Eff}(E)$ trends. Excitations at high (purple), moderate (blue), and low (red) photon energies, indicated as upward arrows, are superimposed on a generic schematic of quantum-confinement states within the CB (gray) of an NP. Intraband relaxation of excited electrons to the lowest-energy CB state is depicted by downward arrows. The role of each type of electron trap that could contribute to the $PL_{Eff}(E)$ spectra is illustrated at the right in the corresponding panel. The points on the $PL_{Eff}(E)$ spectra indicate the values that would be measured with excitation at each arrow. The panels illustrate (a) a continuum of trap states spanning the entire CB region, (b) a discrete number of charge-transfer traps that would be sampled during relaxation, and (c) a discrete number of optically coupled charge-transfer traps that would only be accessed during photoexcitation.

result in a monotonically decreasing PL efficiency with excitation energy. The schematic shown is for electrons in the CB, but a similar diagram would be appropriate for holes in the VB. Quantum-confinement states within the CB (black horizontal lines) of the semiconductor NP are energetically overlapped by a continuum of electron traps (black rectangle), which are likely on the surface of the NP. These traps would remove photogenerated electrons from the semiconductor CB at any energy and reduce the probability for relaxation of electrons to the band edge. Excitation of the electron just above the band edge (short red arrow) would sample only a small energetic range of the traps during relaxation to the band edge, and the Φ_{PL} value would be only slightly reduced. For higher photoexcitation energies (blue and purple arrows), the electron would be promoted to higher-energy quantumconfinement states within the semiconductor CB. The total number of traps accessible during intraband relaxation of the electron would increase at these excitation energies. As a result, the probability that the electron would reach the band edge and the ensemble Φ_{PL} would decrease with increasing excitation energy. This type of carrier trapping is consistent with the decreasing efficiencies in the $\Phi_{PL}(E)$ and $PL_{Eff}(E)$ spectra with increasing excitation energy and the independence of the τ_{AVG} values on excitation energy.

A scenario of energetically discrete traps within the CB is illustrated in Figure 3b. The photoexcited electron would become trapped during intraband relaxation only when it is at the same energy as one of the traps. In general, the total number of traps sampled during relaxation would increase and the $\Phi_{\rm PL}$ would decrease at higher excitation energies. If a ${\rm PL}_{\rm Eff}(E)$ spectrum was recorded for an NP sample with these energetically localized electron traps, an EED that decreases in a steplike fashion with increasing energy would be observed. We did not observe this type of EED for any of the samples investigated.

A different scenario that would yield local minima in the $PL_{Eff}(E)$ spectrum of an NP, which is commonly observed, is

illustrated in Figure 3c. Here there are energetically localized traps or channels for nonradiative pathways that can be accessed only with optical excitation at that energy. An electron excited to an energy not resonant with one of these traps would relax to the band edge with perfect efficiency. Thus, the $\mathrm{PL}_{\mathrm{Eff}}(E)$ spectrum for an NP with optically coupled traps would be constant except at the energies of the traps, where there would be dips or minima. This type of optically coupled carrier trapping would also yield τ_{AVG} values that do not change with excitation energy.

The $PL_{Eff}(E)$ spectra of the CdSe QDs and QPs (Figure 1a,b) suggest that the NPs in each sample have a continuum of traps and multiple localized, optically coupled trap states present on their surfaces. The energies of these discrete traps tend to be away from the transition energies associated with transitions between quantum-confinement states (Table SI). Instead, they tend to be in energetic regions with a lower DOS for these NPs. The as-synthesized CdTe QWs (Figure 1c) have a very low Φ_{PL} at all energies, and they also have multiple localized, optically coupled traps that compete with intraband relaxation. It should be noted that the energies of the minima in this $PL_{Eff}(E)$ spectrum seem to shift relative to the maxima in the absorption spectrum (dotted lines). As can be seen in Figure 1c, the minima near 1.95 and 2.22 eV are just below the absorption peaks at ~2.01 and ~2.29 eV, but the minimum at \sim 2.52 eV is nearly isoenergetic with the maximum of the $1\Phi/$ $2\Sigma/1\Gamma$ absorption feature at ~2.52 eV. As a result, we do not associate the minima with the excitonic transitions. Lastly, the poor overall PL efficiency of these CdTe QWs likely results from nonradiative dynamics of the carriers at the band edge. The enhancement of the CdTe QWs resulted in a dramatic increase in the emission efficiency at all excitation energies, and the nature of the surface traps changed. The $PL_{Eff}(E)$ spectrum for the enhanced CdTe QWs (Figure 1d) suggests that there is a continuum of surface trap states, particularly at higher energies, that competes with relaxation of the carriers to the band edge. There are no obvious local minima in this $PL_{Eff}(E)$ spectrum.

The surface chemistry of the NPs appears to play significant roles in determining the dynamics of photogenerated charge carriers and the EED of the PL efficiency. This is illustrated by comparing the $PL_{Eff}(E)$ spectra of the CdTe QWs included in Figure 1c,d. The postsynthetic treatment of the CdTe QWs increases the Φ_{PL} values of the QWs and changes the properties of the $PL_{Eff}(E)$ spectrum. These results are consistent with those reported by Hoy et al.²³ on QDs. In that Letter, the $PL_{Eff}(E)$ spectrum of a sample of CdSe QDs contained both localized minima and a decreasing efficiency with excitation energy, similar to that shown in Figure 1a. In contrast, there were no minima present, just a monotonically decreasing efficiency with excitation energy, in the $PL_{Eff}(E)$ spectrum of a sample of CdSe/ZnS QDs.²³ The Φ_{PL} values of the CdSe/ZnS QDs were notably higher than those of the core-only CdSe QDs, and the energetically localized, optically coupled traps were removed in the core/shell heterostructure.

The discrete optically coupled traps attributed to the local minima observed in the $PL_{Eff}(E)$ spectra of several of these NPs could arise from multiple types of semiconductor-surface molecule interactions. Numerous reports have indicated the presence of such resonances in the excitation spectra of semiconductor QDs, 49-55 and most of these agree that the coupling mechanism is similar to the metal-ligand coupling associated with surface-enhanced Raman scattering (SERS).⁵ The coupling equation implemented for characterizing the polarizability or SERS spectrum contains three resonance terms in the denominator: one for Mie scattering, one for charge transfer, and one for exciton resonance (see eq 5 in ref 52). The numerator of the coupling equation includes a product of terms for excitonic electron-hole transitions in the semiconductor, charge-transfer (CT) transitions, and a Herzberg-Teller term that results from breakdown of the Born-Oppenheimer approximation and mixing of the semiconductor and surface molecule vibronic functions. 51,52,56 The strengths of these coupling terms depend on the semiconductor type, the shape of the NP, the specific quantumconfinement states excited, and the surface molecules and their orientations relative to the NP surface. 50-52 Because of the small sizes and volumes of the NPs investigated here, resonances associated with Mie scattering are likely not relevant. As mentioned above, we do not associate the minima in the $PL_{Eff}(E)$ spectra with excitonic transitions. Thus, we focus on the possible role of CT transitions and Herzberg-Teller coupling.

The CT transitions are nonvertical transitions between either the quantum-confinement states in the VB of the semiconductor and unoccupied molecular orbitals of surface ligands or the occupied molecular orbitals of the ligands and states in the CB of the semiconductor. These CT transitions borrow intensity from either surface ligand or excitonic transitions. They result in the enhancement of the NP longitudinal optical phonons as well as vibrational excitation of the surface ligands, which are both observed in Raman spectra of the NPs. A9,50,53,55 Mack et al. Tecorded the Raman spectra of CdSe QDs with several different types of surface-ligand passivation using a single resonant excitation energy. For CdSe QDs passivated with thiophenolate (PhS), they determined that there were enhancements of the a₁ and b₂ Raman modes of the PhS molecule, which lie in the 970–1700

cm⁻¹ window. They also found that the coupling with the ligand vibrational modes is more pronounced for smaller QDs.

The spacings between the minima in the $PL_{Eff}(E)$ spectrum of the CdSe QDs range between 1140 and 1610 cm⁻¹, and those in the CdTe QWs are notably larger, ranging from 1770 to 2400 cm⁻¹. There are no clear energy progressions or frequencies that can be associated with the Raman- or infrared-active vibrational modes of any of the passivating ligands on these NPs. Nevertheless, we propose that the CT transitions that spectrally overlap with the absorption spectra of the NPs result in photoexcitation of fewer electrons or holes in the semiconductor at discrete excitation energies and in minima in the $PL_{Eff}(E)$ spectra. It would be interesting to record the Raman spectra as a function of excitation energy and compare the EED of the intensities of the Raman spectral features with that of the $PL_{Eff}(E)$ to identify the role of CT and the specific vibrational modes involved.

It is important to emphasize that the EED trends reported for each type of NP in Figure 1 are not universal for that NP. Rather, the data presented in this Letter indicate that there is commonly an EED of the PL efficiency for an NP and that it depends on many factors. Consider for instance the $PL_{Eff}(E)$ spectra of CdSe QDs. The $PL_{Eff}(E)$ spectrum of the W CdSe QDs (~4.1 nm diameter) in Figure 4a contrasts with the spectrum collected for slightly larger W CdSe QDs (~5.7 nm diameter) in Figure 1a. The $PL_{Eff}(E)$ spectra of both QD samples contain multiple minima, but the spectrum of the 5.7 nm CdSe QD sample, which has Φ_{PL} = 11.5(4)% at an excitation energy of 2.78 eV, decreases substantially with increasing excitation energy through this spectral region. The EED of the smaller QDs (Figure 4a) does not contain this large drop in efficiency, and it is consistent with the $PL_{Eff}(E)$ spectra reported for CdSe QDs (~2.96 nm diameter).³⁹ The origins of the different EEDs for these CdSe QD samples are not clear, but we have found that the handling of the same sample during preparation can result in similar differences in the trends.

Figure 4b,c shows the spectral data for samples of W CdSe QBs (~1.8 nm thick) dispersed in toluene and dichloromethane, respectively. The absorption spectra for these pseudo-1D QBs are nearly identical to those of the W CdSe QPs plotted in Figure 1b since the thickness of these NPs, ~1.8 nm, dominates the quantum-confinement energies and transition strengths. The PL(E) spectra of the CdSe QBs suspended in the two solvents have similar tails extending to lower energies, a feature commonly associated with trap states below the band edge. There is a measurable dependence of the Stokes shift of the PL maximum on the solvent for these CdSe QBs; the Stokes shifts are ~54 and ~30 meV for the QBs in toluene and dichloromethane, respectively. The two samples have nearly identical Φ_{PL} values of 0.20(1)% and 0.22(1)% measured at an excitation energy of 3.14 eV, which is where the $PL_{Eff}(E)$ spectra are normalized to unity. Despite the similar Φ_{PL} values, there are a couple of noticeable differences between the $PL_{Eff}(E)$ spectra. Both $PL_{Eff}(E)$ spectra have a minimum near the energy of the 1_e-1A absorption feature, but the minimum is more pronounced for the dichloromethane sample. In addition, the efficiency of the sample in toluene decreases with increasing energy, but the efficiency measured for the CdSe QBs in dichloromethane remains nearly constant. These observed differences for the same CdSe QBs suspended in different solvents could be due to contrasting surface passivation induced by the solvents, but the overall similar $\Phi_{\rm PL}$

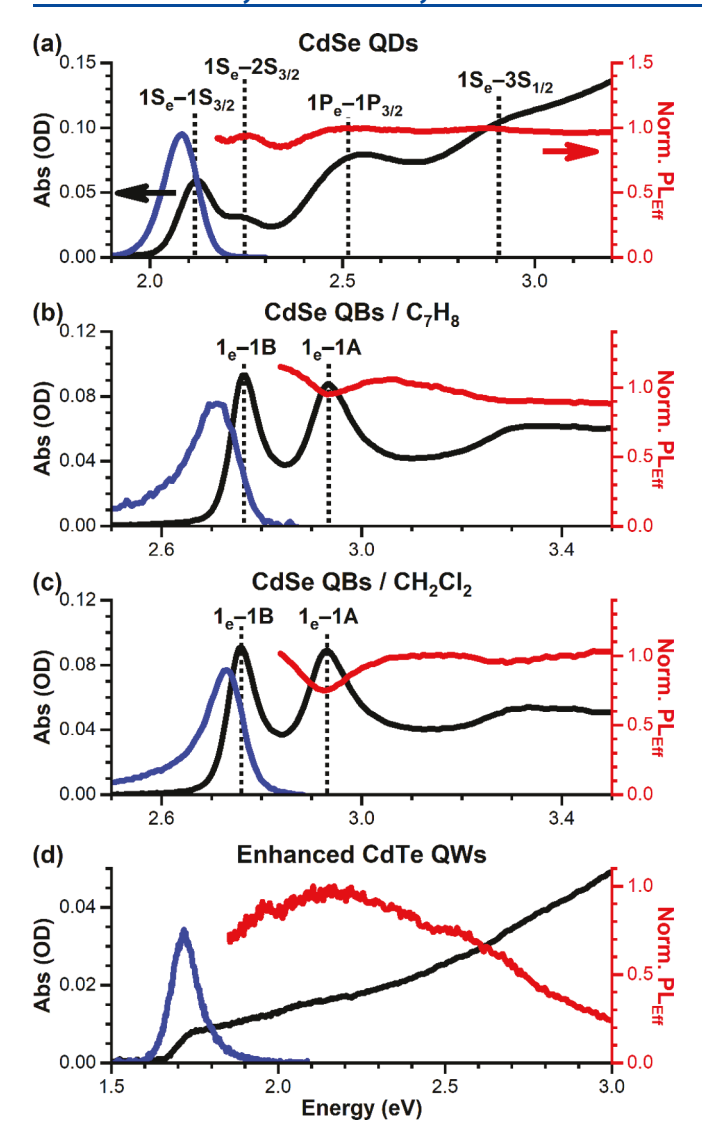


Figure 4. Abs(E) (black), PL(E) (blue), and PL_{Eff}(E) (red) spectra for (a) W CdSe QDs (\sim 4.1 nm diameter) in toluene, (b) W CdSe QBs (\sim 1.8 nm thick) in toluene, (c) W CdSe QBs (\sim 1.8 nm thick) in dichloromethane, and (d) enhanced W CdTe QWs (\sim 7.5 nm diameter) in tri-n-octylphosphine, which exhibit different EED trends. Peaks in the absorption spectra are indicated with dotted lines and labeled.

values suggest otherwise. Instead, we deduce that it is the solvent itself that gives rise to these differences in the EED trends.

Lastly, the surface passivation of the CdTe QWs also gives rise to changes in the EED. The $PL_{Eff}(E)$ spectrum for the enhanced ZB/W CdTe QWs (7.4 nm diameter and Φ_{PL} = 13.5% measured at 1.922 eV), shown in Figure 1d, has a small rise, an overall maximum just above 1.9 eV, and then a decrease in efficiency with increasing excitation. A sample of W CdTe QWs (~7.5 nm diameter) was enhanced in a similar manner, reaching Φ_{PL} = 25(3)% at an excitation energy of 2.12 eV. The $PL_{Eff}(E)$ spectrum for this sample (Figure 4d) has a steeper rise to a maximum near 2.16 eV and then a slightly faster decrease in efficiency with excitation energy. Thus, while the maximum value of the Φ_{PL} is higher for this second sample, the shape changed. In fact, if the Φ_{PL} had been measured for this sample at an excitation energy of 1.922 eV, it would be

~20%, a bit closer to the value measured for the first sample. During the enhancement process, it is primarily the surface of the CdTe QWs that is being changed with the addition of a CdS monolayer on the surface, ⁴⁶ and this reduces the number of traps and nonradiative pathways that can be sampled.

In summary, the PL efficiencies of semiconductor NPs typically have a dependence on the excitation energy. The details of the EED trends do not appear to depend on the dimensionality of the NP. Instead, the trends seem to depend significantly on the nature of the surface of the NP. A majority of the samples investigated have energetically localized minima in the $PL_{Eff}(E)$ spectra at excitation energies that lie between the maxima of the absorption features. We propose that these local minima arise from excitation of charge carriers into optically coupled surface trap states with likely contributions from CT transitions. An overall decrease in the radiative efficiency with increasing excitation energy was also observed for a majority of samples. This EED trend is attributed to the presence of a continuum of nonradiative carrier traps that can be accessed during intraband relaxation of the carriers to the band edge. Two samples of enhanced CdTe QWs also exhibited increasing emission efficiency with increasing excitation energy just above the band edge. This trend is associated with a continuum of optically coupled traps at lower excitation energies that decreases in density with increasing energy. We conclude that the roles of the nonradiative pathways, especially those of the optically coupled trap states, are largely dictated by the surfaces of the NPs and the ligands on their surfaces. It also appears as though the solvent in which the NPs are suspended can also contribute to the properties of the $PL_{Eff}(E)$ spectrum. The data presented do emphasize the importance of reporting the excitation energy when probing photoluminescence quantum yields or dynamics and of characterizing the EED of semiconductor NP samples.

ASSOCIATED CONTENT

Supporting Information

The Supporting Information is available free of charge at https://pubs.acs.org/doi/10.1021/acs.jpclett.0c00489.

Details of the synthesis of the semiconductor NPs, optical spectroscopy details, determination of energies of local maxima and minima in the spectra, comparisons of $\Phi_{\rm Eff}(E)$ and $\Phi_{\rm PL}(E)$ spectra, and PL lifetime profiles and analyses (PDF)

AUTHOR INFORMATION

Corresponding Author

Richard A. Loomis — Department of Chemistry and Institute of Materials Science and Engineering, Washington University in St. Louis, Saint Louis, Missouri 63130, United States; orcid.org/0000-0002-3172-6336; Email: loomis@wustl.edu

Authors

William M. Sanderson — Department of Chemistry and Institute of Materials Science and Engineering, Washington University in St. Louis, Saint Louis, Missouri 63130, United States; orcid.org/0000-0001-5346-1730

Jessica Hoy — Department of Chemistry and Institute of Materials Science and Engineering, Washington University in St. Louis, Saint Louis, Missouri 63130, United States;
orcid.org/0000-0002-4392-8939

- Calynn Morrison Department of Chemistry and Institute of Materials Science and Engineering, Washington University in St. Louis, Saint Louis, Missouri 63130, United States;
 orcid.org/0000-0002-0952-3444
- Fudong Wang Department of Chemistry and Institute of Materials Science and Engineering, Washington University in St. Louis, Saint Louis, Missouri 63130, United States;
 orcid.org/0000-0003-2914-1360
- Yuanyuan Wang Department of Chemistry and Institute of Materials Science and Engineering, Washington University in St. Louis, Saint Louis, Missouri 63130, United States
- Paul J. Morrison Department of Chemistry and Institute of Materials Science and Engineering, Washington University in St. Louis, Saint Louis, Missouri 63130, United States
- William E. Buhro Department of Chemistry and Institute of Materials Science and Engineering, Washington University in St. Louis, Saint Louis, Missouri 63130, United States;

 orcid.org/0000-0002-7622-4145

Complete contact information is available at: https://pubs.acs.org/10.1021/acs.jpclett.0c00489

Author Contributions

[†]W.M.S. and J.H. contributed equally to this work.

Notes

The authors declare no competing financial interest.

ACKNOWLEDGMENTS

This work was supported by the NSF under Grants DMR-1611149 and DMR-1905751 (R.A.L.) and CHE-1607862 (W.E.B.).

■ REFERENCES

- (1) Murray, C. B.; Norris, D. J.; Bawendi, M. G. Synthesis and Characterization of Nearly Monodisperse CdE (E = S, Se, Te) Semiconductor Nanocrystallites. *J. Am. Chem. Soc.* **1993**, *115*, 8706–8715
- (2) Zorman, B.; Ramakrishna, M. V.; Friesner, R. A. Quantum Confinement Effects in CdSe Quantum Dots. *J. Phys. Chem.* **1995**, *99*, 7649–7653
- (3) Yoffe, A. D. Semiconductor Quantum Dots and Related Systems: Electronic, Optical, Luminescence and Related Properties of Low Dimensional Systems. *Adv. Phys.* **2001**, *50*, 1–208.
- (4) Qu, L.; Peng, X. Control of Photoluminescence Properties of CdSe Nanocrystals in Growth. *J. Am. Chem. Soc.* **2002**, *124*, 2049–2055
- (5) Burda, C.; Chen, X.; Narayanan, R.; El-Sayed, M. A. Chemistry and Properties of Nanocrystals of Different Shapes. *Chem. Rev.* **2005**, 105, 1025–1102.
- (6) Ramasamy, P.; Kim, N.; Kang, Y.-S.; Ramirez, O.; Lee, J.-S. Tunable, Bright, and Narrow-Band Luminescence from Colloidal Indium Phosphide Quantum Dots. *Chem. Mater.* **2017**, *29*, 6893–6899.
- (7) Sanderson, W. M.; Schrier, J.; Loomis, R. A. Photo-Induced State Shifting in Semiconductor Quantum Nanoparticles. *Nano Lett.* **2020**, submitted.
- (8) Kambhampati, P. On the Kinetics and Thermodynamics of Excitons at the Surface of Semiconductor Nanocrystals: Are There Surface Excitons? *Chem. Phys.* **2015**, *446*, 92–107.
- (9) Underwood, D. F.; Kippeny, T.; Rosenthal, S. J. Ultrafast Carrier Dynamics in CdSe Nanocrystals Determined by Femtosecond Fluorescence Upconversion Spectroscopy. *J. Phys. Chem. B* **2001**, *105*, 436–443.
- (10) Krause, M. M.; Kambhampati, P. Linking Surface Chemistry to Optical Properties of Semiconductor Nanocrystals. *Phys. Chem. Chem. Phys.* **2015**, *17*, 18882–18894.

- (11) Palato, S.; Seiler, H.; McGovern, L.; Mack, T. G.; Jethi, L.; Kambhampati, P. Electron Dynamics at the Surface of Semiconductor Nanocrystals. *J. Phys. Chem. C* **2017**, *121*, 26519–26527.
- (12) Yao, Y.; DeKoster, G. T.; Buhro, W. E. Interchange of L-, Z-, and Bound-Ion-Pair X-Type Ligation on Cadmium Selenide Quantum Belts. *Chem. Mater.* **2019**, *31*, 4299–4312.
- (13) Busby, E.; Anderson, N. C.; Owen, J. S.; Sfeir, M. Y. Effect of Surface Stoichiometry on Blinking and Hole Trapping Dynamics in CdSe Nanocrystals. *J. Phys. Chem. C* **2015**, *119*, 27797–27803.
- (14) Cheng, C.-Y.; Mao, M.-H. Photo-Stability and Time-Resolved Photoluminescence Study of Colloidal CdSe/ZnS Quantum Dots Passivated in Al₂O₃ Using Atomic Layer Deposition. *J. Appl. Phys.* **2016**, *120*, 083103.
- (15) Peterson, M. D.; Cass, L. C.; Harris, R. D.; Edme, K.; Sung, K.; Weiss, E. A. The Role of Ligands in Determining the Exciton Relaxation Dynamics in Semiconductor Quantum Dots. *Annu. Rev. Phys. Chem.* **2014**, *65*, 317–339.
- (16) De, C. K.; Routh, T.; Roy, D.; Mandal, S.; Mandal, P. K. Highly Photoluminescent InP Based Core Alloy Shell QDs from Air-Stable Precursors: Excitation Wavelength Dependent Photoluminescence Quantum Yield, Photoluminescence Decay Dynamics, and Single Particle Blinking Dynamics. *J. Phys. Chem. C* **2018**, *122*, 964–973.
- (17) Novak, S.; Scarpantonio, L.; Novak, J.; Prè, M. D.; Martucci, A.; Musgraves, J. D.; McClenaghan, N. D.; Richardson, K. Incorporation of Luminescent CdSe/ZnS Core-Shell Quantum Dots and PbS Quantum Dots into Solution-Derived Chalcogenide Glass Films. *Opt. Mater. Express* **2013**, *3*, 729–738.
- (18) Moroz, P.; Liyanage, G.; Kholmicheva, N. N.; Yakunin, S.; Rijal, U.; Uprety, P.; Bastola, E.; Mellott, B.; Subedi, K.; Sun, L.; Kovalenko, M. V.; Zamkov, M. Infrared Emitting PbS Nanocrystal Solids through Matrix Encapsulation. *Chem. Mater.* **2014**, *26*, 4256–4264.
- (19) Blackman, B.; Battaglia, D.; Peng, X. Bright and Water-Soluble Near IR-Emitting CdSe/CdTe/ZnSe Type-II/Type-I Nanocrystals, Tuning the Efficiency and Stability by Growth. *Chem. Mater.* **2008**, 20, 4847–4853.
- (20) Greytak, A. B.; Allen, P. M.; Liu, W.; Zhao, J.; Young, E. R.; Popović, Z.; Walker, B. J.; Nocera, D. G.; Bawendi, M. G. Alternating Layer Addition Approach to CdSe/CdS Core/Shell Quantum Dots with Near-Unity Quantum Yield and High On-Time Fractions. *Chem. Sci.* 2012, 3, 2028–2034.
- (21) Chen, O.; Zhao, J.; Chauhan, V. P.; Cui, J.; Wong, C.; Harris, D. K.; Wei, H.; Han, H.-S.; Fukumura, D.; Jain, R. K.; Bawendi, M. G. Compact High-Quality CdSe–CdS Core–Shell Nanocrystals with Narrow Emission Linewidths and Suppressed Blinking. *Nat. Mater.* **2013**, *12*, 445.
- (22) Saha, A.; Chellappan, K. V.; Narayan, K. S.; Ghatak, J.; Datta, R.; Viswanatha, R. Near-Unity Quantum Yield in Semiconducting Nanostructures: Structural Understanding Leading to Energy Efficient Applications. J. Phys. Chem. Lett. 2013, 4, 3544–3549.
- (23) Hoy, J.; Morrison, P. J.; Steinberg, L. K.; Buhro, W. E.; Loomis, R. A. Excitation Energy Dependence of the Photoluminescence Quantum Yields of Core and Core/Shell Quantum Dots. *J. Phys. Chem. Lett.* **2013**, *4*, 2053–2060.
- (24) Samokhvalov, P.; Linkov, P.; Michel, J.; Molinari, M.; Nabiev, I. Photoluminescence Quantum Yield of CdSe-ZnS/CdS/ZnS Core-Multishell Quantum Dots Approaches 100% Due to Enhancement of Charge Carrier Confinement. *Proc. SPIE* 2014, 8955, 89550S.
- (25) Tessier, M. D.; Spinicelli, P.; Dupont, D.; Patriarche, G.; Ithurria, S.; Dubertret, B. Efficient Exciton Concentrators Built from Colloidal Core/Crown CdSe/CdS Semiconductor Nanoplatelets. *Nano Lett.* **2014**, *14*, 207–213.
- (26) Pedetti, S.; Ithurria, S.; Heuclin, H.; Patriarche, G.; Dubertret, B. Type-II CdSe/CdTe Core/Crown Semiconductor Nanoplatelets. *J. Am. Chem. Soc.* **2014**, *136*, 16430–16438.
- (27) Linkov, P.; Krivenkov, V.; Nabiev, I.; Samokhvalov, P. High Quantum Yield CdSe/ZnS/CdS/ZnS Multishell Quantum Dots for Biosensing and Optoelectronic Applications. *Mater. Today: Proc.* **2016**, *3*, 104–108.

- (28) Guyot-Sionnest, P.; Shim, M.; Matranga, C.; Hines, M. Intraband Relaxation in CdSe Quantum Dots. *Phys. Rev. B: Condens. Matter Mater. Phys.* **1999**, *60*, R2181.
- (29) Bockelmann, U.; Bastard, G. Phonon Scattering and Energy Relaxation in Two-, One-, and Zero-Dimensional Electron Gases. *Phys. Rev. B: Condens. Matter Mater. Phys.* **1990**, 42, 8947–8951.
- (30) Xu, S.; Mikhailovsky, A. A.; Hollingsworth, J. A.; Klimov, V. I. Hole Intraband Relaxation in Strongly Confined Quantum Dots: Revisiting the "Phonon Bottleneck" Problem. *Phys. Rev. B: Condens. Matter Mater. Phys.* **2002**, *65*, 045319.
- (31) Cooney, R. R.; Sewall, S. L.; Anderson, K. E. H.; Dias, E. A.; Kambhampati, P. Breaking the Phonon Bottleneck for Holes in Semiconductor Quantum Dots. *Phys. Rev. Lett.* **2007**, *98*, 177403.
- (32) Klimov, V. I.; Mikhailovsky, A. A.; McBranch, D. W.; Leatherdale, C. A.; Bawendi, M. G. Mechanisms for Intraband Energy Relaxation in Semiconductor Quantum Dots: The Role of Electron-Hole Interactions. *Phys. Rev. B: Condens. Matter Mater. Phys.* **2000**, *61*, R13349.
- (33) Klimov, V. I.; McBranch, D. W. Femtosecond 1P-to-1S Electron Relaxation in Strongly Confined Semiconductor Nanocrystals. *Phys. Rev. Lett.* **1998**, *80*, 4028–4031.
- (34) Klimov, V. I. Optical Nonlinearities and Ultrafast Carrier Dynamics in Semiconductor Nanocrystals. *J. Phys. Chem. B* **2000**, *104*, 6112–6123.
- (35) Guyot-Sionnest, P.; Wehrenberg, B.; Yu, D. Intraband Relaxation in CdSe Nanocrystals and the Strong Influence of the Surface Ligands. *J. Chem. Phys.* **2005**, *123*, 074709.
- (36) Kuno, M.; Ahmad, O.; Protasenko, V.; Bacinello, D.; Kosel, T. H. Solution-Based Straight and Branched CdTe Nanowires. *Chem. Mater.* **2006**, *18*, 5722–5732.
- (37) Hoheisel, W.; Colvin, V. L.; Johnson, C. S.; Alivisatos, A. P. Threshold for Quasicontinuum Absorption and Reduced Luminescence Efficiency in CdSe Nanocrystals. *J. Chem. Phys.* **1994**, *101*, 8455–8460.
- (38) Li, B.; Brosseau, P. J.; Strandell, D. P.; Mack, T. G.; Kambhampati, P. Photophysical Action Spectra of Emission from Semiconductor Nanocrystals Reveal Violations to the Vavilov Rule Behavior from Hot Carrier Effects. *J. Phys. Chem. C* **2019**, *123*, 5092–5098.
- (39) Mooney, J.; Krause, M. M.; Kambhampati, P. Connecting the Dots: The Kinetics and Thermodynamics of Hot, Cold, and Surface-Trapped Excitons in Semiconductor Nanocrystals. *J. Phys. Chem. C* **2014**, *118*, 7730–7739.
- (40) Martynenko, I. V.; Baimuratov, A. S.; Osipova, V. A.; Kuznetsova, V. A.; Purcell-Milton, F.; Rukhlenko, I. D.; Fedorov, A. V.; Gun'ko, Y. K.; Resch-Genger, U.; Baranov, A. V. Excitation Energy Dependence of the Photoluminescence Quantum Yield of Core/Shell CdSe/CdS Quantum Dots and Correlation with Circular Dichroism. *Chem. Mater.* 2018, 30, 465–471.
- (41) Chung, H.; Choi, H.; Kim, D.; Jeong, S.; Kim, J. Size Dependence of Excitation-Energy-Related Surface Trapping Dynamics in PbS Quantum Dots. *J. Phys. Chem. C* **2015**, *119*, 7517–7524.
- (42) Righetto, M.; Minotto, A.; Bozio, R. Bridging Energetics and Dynamics of Exciton Trapping in Core—Shell Quantum Dots. *J. Phys. Chem. C* **2017**, *121*, 896—902.
- (43) Roy, D.; Das, A.; De, C. K.; Mandal, S.; Bangal, P. R.; Mandal, P. K. Why Does the Photoluminescence Efficiency Depend on Excitation Energy in Case of a Quantum Dot? A Case Study of CdSe-Based Core/Alloy Shell/Shell Quantum Dots Employing Ultrafast Pump—Probe Spectroscopy and Single Particle Spectroscopy. *J. Phys. Chem. C* 2019, 123, 6922—6933.
- (44) Teunis, M. B.; Johnson, M. A.; Muhoberac, B. B.; Seifert, S.; Sardar, R. Programmable Colloidal Approach to Hierarchical Structures of Methylammonium Lead Bromide Perovskite Nanocrystals with Bright Photoluminescent Properties. *Chem. Mater.* **2017**, 29, 3526–3537.
- (45) Nazzal, A. Y.; Wang, X.; Qu, L.; Yu, W.; Wang, Y.; Peng, X.; Xiao, M. Environmental Effects on Photoluminescence of Highly

- Luminescent CdSe and CdSe/ZnS Core/Shell Nanocrystals in Polymer Thin Films. *J. Phys. Chem. B* **2004**, *108*, 5507–5515.
- (46) Liu, Y.-H.; Wang, F.; Hoy, J.; Wayman, V. L.; Steinberg, L. K.; Loomis, R. A.; Buhro, W. E. Bright Core—Shell Semiconductor Quantum Wires. J. Am. Chem. Soc. 2012, 134, 18797—18803.
- (47) Sun, J. W.; Buhro, W. E.; Wang, L. W.; Schrier, J. Electronic Structure and Spectroscopy of Cadmium Telluride Quantum Wires. *Nano Lett.* **2008**, *8*, 2913–2919.
- (48) Olshansky, J. H.; Ding, T. X.; Lee, Y. V.; Leone, S. R.; Alivisatos, A. P. Hole Transfer from Photoexcited Quantum Dots: The Relationship between Driving Force and Rate. *J. Am. Chem. Soc.* **2015**, *137*, 15567–15575.
- (49) Wang, Y.; Zhang, J.; Jia, H.; Li, M.; Zeng, J.; Yang, B.; Zhao, B.; Xu, W.; Lombardi, J. R. Mercaptopyridine Surface-Functionalized CdTe Quantum Dots with Enhanced Raman Scattering Properties. *J. Phys. Chem. C* **2008**, *112*, 996–1000.
- (50) Islam, S. K.; Sohel, M. A.; Lombardi, J. R. Coupled Exciton and Charge-Transfer Resonances in the Raman Enhancement of Phonon Modes of CdSe Quantum Dots (QDs). *J. Phys. Chem. C* **2014**, *118*, 19415–19421.
- (51) Lombardi, J. R.; Birke, R. L. Theory of Surface-Enhanced Raman Scattering in Semiconductors. *J. Phys. Chem. C* **2014**, *118*, 11120–11130.
- (52) Lombardi, J. R. The Theory of Surface-Enhanced Raman Scattering on Semiconductor Nanoparticles; toward the Optimization of SERS Sensors. *Faraday Discuss.* **2017**, 205, 105–120.
- (53) Lifshitz, E. Evidence in Support of Exciton to Ligand Vibrational Coupling in Colloidal Quantum Dots. *J. Phys. Chem. Lett.* **2015**, *6*, 4336–4347.
- (54) Noblet, T.; Dreesen, L.; Boujday, S.; Méthivier, C.; Busson, B.; Tadjeddine, A.; Humbert, C. Semiconductor Quantum Dots Reveal Dipolar Coupling from Exciton to Ligand Vibration. *Commun. Chem.* **2018**, *1*, 76.
- (55) Mack, T. G.; Jethi, L.; Andrews, M.; Kambhampati, P. Direct Observation of Vibronic Coupling between Excitonic States of CdSe Nanocrystals and Their Passivating Ligands. *J. Phys. Chem. C* **2019**, 123, 5084–5091.
- (56) Albrecht, A. C. On the Theory of Raman Intensities. *J. Chem. Phys.* **1961**, 34, 1476–1484.
- (57) Onwudiwe, D. C.; Hrubaru, M.; Ebenso, E. E. Synthesis, Structural and Optical Properties of TOPO and HDA Capped Cadmium Sulphide Nanocrystals, and the Effect of Capping Ligand Concentration. *J. Nanomater.* **2015**, 2015, 143632.